Synthesis and Characterization of Novel Polyimide/SiO_2 Nanocomposite Materials Containing Phenylphosphine Oxide via Sol-Gel Technique

Canan Kizilkaya, Sevim Karataş, Nilhan-Kayaman Apohan, Atilla Güngör

Department of Chemistry, Marmara University, Göztepe, Istanbul 34722, Turkey

Received 17 September 2008; accepted 4 April 2009
DOI 10.1002/app.31404
Published online 3 November 2009 in Wiley InterScience (www.interscience.wiley.com).

ABSTRACT: In this article, a series of novel polyimide/silica (PI/SiO_2) nanocomposite coating materials were prepared from tetraethoxysilane (TEOS), γ-glycidyloxypropyltrimethoxysilane (GOTMS), and polyamic acid (PAA) via sol-gel technique. PAA was prepared by the reaction of 3,3′,4,4′-benzophenone tetracarboxylic dianhydride (BTDA) and bis (3-aminophenyl) phenyphosphine oxide (BAPPO) in *N*-methyl-2- pyrrolidone (NMP). BAPPO was synthesized hydrogenation of bis (3-nitrophenyl) phenyphosphine oxide (BNPPO) in the presence of Pd/C. The silica content in the hybrid coating materials was varied from 0 to 20 wt %. The molecular structures of the composite materials were analyzed by means of FT-IR and ^{29}Si-NMR spectroscopy techniques. The physical and mechanical properties of the nanocomposites were evaluated by various techniques such as, hardness, contact angle, and optical transmission and tensile tests. These measurements revealed that all the properties of the nanocomposite coatings were improved noticeable, by the addition of sol-gel precursor into the coating formulation. Thermogravimetric analysis showed that the incorporation of sol-gel precursor into the polyimide matrix leads to an enhancement in the thermal stability and also flame resistance properties of the coating material. The surface morphology of the hybrid coating was characterized by scanning electron microscopy (SEM). SEM studies indicated that nanometer-scaled inorganic particles were homogenously dispersed throughout the polyimide matrix © 2009 Wiley Periodicals, Inc. J Appl Polym Sci 115: 3256–3264, 2010

Key words: coatings; flame retardance; nanocomposite; polyimides; thin films

INTRODUCTION

Polyimides (PIs) have been well-known high-performance polymer materials due to their outstanding properties such as thermal-oxidative stability, mechanical properties, and good resistance to solvents.[1–3] For that reason, they have found many technological applications in the aerospace, microelectronic, and other advanced technologies.[4] In addition, PIs have been considered as suitable polymer matrix materials for preparation of advanced hybrid composites.

Organic-inorganic nanocomposite materials prepared by the sol-gel technique are an important class of new-generation materials, which combine the desirable properties of an inorganic component (heat resistance, retention of mechanical properties at high temperatures, and low thermal expansion) and those of organic polymer (toughness, ductility, and processability).[5–8] Therefore, polyimide/silica (PI/SiO_2) hybrid materials have attracted particular interest.

The sol-gel technique is one of the most widely used approache for the preparation of PI/SiO_2 nanocomposites where silica particles are dispersed in a polyimide matrix. This method is composed of two step reactions: the hydrolysis of a metal alkoxide in order to produce hydroxyl groups, their followed by the polycondensation of the hydroxyl groups and residual hydroxyl groups to form a three dimensional network. These reactions are typically catalyzed by an acid or base and they occur concurrently. Polyimides are especially suitable for this type of process since they can be produced from polyamic acid (PAA) precursors, which can tolerate the addition of water in order to accomplish the hydrolysis of the metal alkoxide.[9,10] Moreover, since the imidization reaction for the conversion of the PAA to the corresponding polyimide is an intramolecular process, it is not adversely affected by the surrounding inorganic domains.[11] At the same time, the excellent thermal stability of polyimides makes it possible to use high temperatures for the enhancement of the silica network (up to 350°C) without causing any degradation of the organic phase. However, one of the primary problems for

Correspondence to: A. Güngör (atillag_1@yahoo.com).
Contract grant sponsor: Commission of Scientific Research Project, Marmara University; contract grant number: FEN-BGS-290506, 2006.

preparing the PI/SiO_2 hybrid nanocomposite materials is the phase separation between the polyimide matrix and inorganic moieties. To overcome the phase separation of between polyimide and inorganic metal alkoxide, the approach of either short chain polyimide segment, coupling agents or the combination of both approaches were used to improve the compatibility by increasing the density of coupling sites.[12–16]

So far, a number of studies have been conducted for preparation and characterization of hybrid materials based on PI/SiO_2. Huang and Gu reported a series of PI/SiO2 hybrids with silica contents up to 30 wt % were successfully prepared by the sol-gel reaction.[17] The results indicated that the decomposition temperatures and the glass-transition temperatures (T_g) of the polyimide based hybrid materials increased with increasing silica content. Furthermore, it was observed that the tensile strength of the hybrids reached a maximum value when the silica content was up to 11 wt %. Wang et al.[18] have studied the synthesis and characterization of the organosoluble PI/SiO_2 nanocomposite materials prepared from 4,4′-oxydipthalic dianhydride (ODPA) and 4,4′diamino-3,3′-dimethyldiphenylmethane (DMM DA). It was found that the silica particle size in the polymide matrix is in the range of 40–100 nm when the silica content is less than 20 wt %. Furthermore, the modulus and strength of the hybrid materials were improved due to the fact that the degree of crosslinking increased with increasing the amount of the alkoxysilane. Park et al.[19] prepared poly(imide siloxane)-silica hybrids from the siloxane-containing poly(amic acid) and tetraethoxysilane (TEOS). They investigated the effects of polydimethylsiloxane (PDMS) as a compatibilizer in the hybrid system. Musto et al.[20] reported that the molecular structure of the silica phase in the hybrid system was strongly dependent on the presence the γ-glycidyloxypropyltrimethoxysilane (GOTMS) as a coupling agent due to a reduction on the rate of particle–growth. Ahmad and coworkers prepared PI/SiO_2 nano hybrid materials from poly (hydroxy amic acid) and TEOS.[21] It was demonstrated that the pendant hydroxyl groups on the polyimide chain prevented the agglomeration of silica particles due to reducing the particle size and making their dispersion more homogenous in the matrix. Zhong et al.[22] reported that PI-silica hybrid membranes exhibited excellent gas permeabilities and hydrophilic properties. Cornelius and Marand reported that a series of PI-silica composites were manufactured from a functionalized fluorinated polyimide and various alkoxysilane compounds via sol-gel method.[23] It was found that the morphology of the hybrid materials was greatly dependent on the type of alkoxide precursor employed in the hybrid system.

Polyimides containing phosphine oxide moieties display good flame resistance and excellent adhesion properties. It has been proven that the phenylphosphine oxide moiety provides a strong interacting site for imparting miscibility with several systems.[24–27]

In this study, a series of novel PI/SiO_2 nanocomposite materials containing phenyphosphine oxide group were prepared via the sol-gel process from pre-hydrolyzed TEOS and poly (amic acid) (PAA) obtained by the reaction between 3,3′,4,4′-benzophenone tetracarboxylic dianhydride (BTDA) and bis (3-aminophenyl) phenyphosphine oxide (BAPPO), GOTMS as a compatibilizer to enhance the interchain interaction of the produced hybrid materials. The molecular structure and morphology of the PI-silica hybrid coating materials were characterized by FTIR and scanning electron microscopy (SEM). To evaluate the coating properties, the hybrid formulations were applied on to glass panels and then imidized by a thermal procedure. Moreover, the mechanical, thermal, and optical properties as well as contact angle and hardness of the nanohybrid coating materials with different silica content were studied and correlated with the molecular structure.

EXPERIMENTAL

Materials

The dianhydride monomer, BTDA (Merck), TEOS (Fluka, Istanbul, Turkey), GOTMS (Merck) were used without further purification. *N*-Methyl-2-pyrrolidone (NMP) (Merck) was dried over phosphorous pentoxide (P_2O_5) and freshly distilled under vacuum before used. Triphenyl phosphineoxide (TPPO) was prepared by oxidation of triphenyl phosphine according to the literature.[28] Hydrochloric acid (32%), nitric acid (70%), sulfuric acid (98%), hydrogen peroxide (30%), and palladium on activated carbon (10% Pd/C) were obtained from Merck. Celite was purchased from Fluka, Turkey. Some common solvents such as; chloroform, ethanol, methanol, dichloroethane were used as received. Glass panels were used in all the coatings (50 mm×100 mm×2 mm).

Synthesis of bis (3-nitrophenyl)phenyl phosphine oxide

The synthesis of bis (3-nitroophenyl)phenylphosphine oxide (BNPPO) has been reported in detail elsewhere.[29,30] Briefly, to a firmly dried three-necked round bottom flask equipped with a reflux condenser, a nitrogen gas inlet, an overhead mechanical stirrer and a dropping funnel were charged with 150 g (0.539 mol) of triphenyl phosphine oxide and placed in an ice-bath. Then, concentrated (98%)

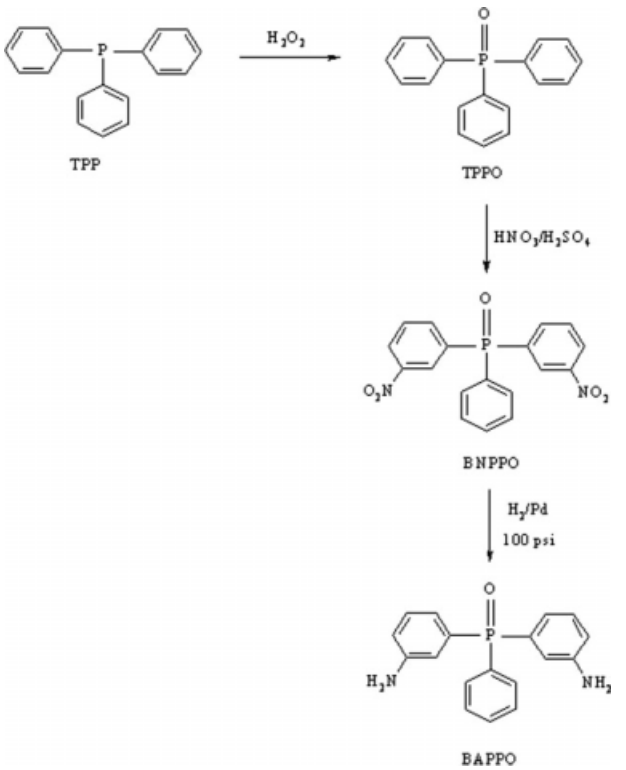

Figure 1 The synthesis route for bis (3-amino phenyl)-phenylphosphine oxide (BAPPO).

sulfuric acid (350 mL) was carefully added to the content of the flask. The mixture was stirred until all starting materials were dissolved. In a separate place, acid mixture was prepared from nitric acid (70%, 97.03 g, 1.078 mol) and sulfuric acid (195 mL). After cooling to 0–5°C, the acid mixture was added dropwise to the triphenyl phosphine oxide solution with in 5 h. Then, the resulting mixture was stirred further 8 h and then precipitated by slowly pouring flask content on crashed ice. The precipitated material was dissolved in dichloride methane and washed with dilute Na_2CO_3 solution until reach to neutral pH. After the dichloride methane removed, the resulting product was crystallized from ethanol three times. The light yellow product was obtained. Yield: 71%. mp: 133°C.

FTIR (KBr):3078 cm^{-1}(aromatic C—H str.), 1610–1573 cm^{-1} aromatic C=C str.), 1350–1525 cm^{-1} asym. and sym. —N=O str., 1191 cm^{-1} (—P=O str.)

^{1}H-NMR (CD3OD): δ 8.50–8.55 ppm (4 H); δ 8.05–8.10 ppm (4H); δ 7.60–7.90 ppm (nonsubstitue aromatic ring 5 H)

Synthesis of bis (3-aminophenyl)phenyl phosphine oxide

Bis (3-aminophenyl)phenylphosphine oxide (BAPPO) was obtained by hydrogenation of bis (3-nitrophenyl)phenyl phenylphosphineoxide (BNPPO) in a high pressure reactor (Parr Instrument Co., USA). 20 g (0.054 mol) of BNPPO, 500 mL of methanol and 0.5 g of Pd/C catalyst were charged into the flame dried pressure reactor. Firstly, the reactor was purged with nitrogen gas for several minutes and then, pressured with hydrogen gas to 100 psi. The reaction mixture was heated at 50°C and allowed to react for 48 h. Next, the reaction mixture was filtered over Celite® in a Buchner funnel under vacuum. The methanol was removed by rotary evaporation and a product with bright light yellow crystals was obtained. This material was crystallized from 1,2-dichloro ethane three times.

FTIR (KBr): 3460 and 3358 cm^{-1} (N—H str.), 1595 cm^{-1} (N—H bend.), 1437 cm^{-1} (aromatic C-P str.) 1199 cm^{-1} (P=O str.).

^{1}H-NMR(CD_3OD): δ 7.75–6.80 ppm (aromatic ring,13H, multiple); 3.2–3.4 ppm (amino group 4H).

Preparation of poly(amic acid) solution

Poly(amic acid) (PAA) used as a polyimide precursor was prepared in NMP as follows: the diamine monomer (BAPPO) and firmly dried NMP were charged into a three neck flask under nitrogen atmosphere. Then, equimolar amount of the dianhydride monomer (BTDA) were incrementally added into the content of the flask. The solid concentration was afforded as 20 (wt/v) %. The reaction mixture was stirred over night at room temperature to obtain a viscous PAA solution.

Preparation of sol-gel precursor

The sol-gel precursor was prepared by using TEOS (8.7 g, 0.0418 mol) and GOTMS (2.25 g, 0.0095 mol) as the precursor alkoxides, ethanol (EtOH) (2.25 g, 0.05 mol) as solvent, (1.763 g, 0.098 mol) distilled water for hydrolysis and (0.075 g) HCl as a catalyst. Initially, TEOS, GOTMS and EtOH were charged into a glass vial and then water that had been acidified by adding HCl was slowly dropped into the vial. The mixture was magnetically stirred at room temperature, until a clear solution was obtained. A slight heat evolution indicated the starting of the exothermic hydrolysis reaction and the silane sol was allowed to stand at room temperature for about 1 h.

Preparation of polyimide/silica nanocomposites materials

To acquire precursor hybrid solution, appropriate amounts of the silane sol were introduced into the PAA solution in a drop wise manner and mixed in a beaker at room temperature for 4 h. After through mixing, the clear and viscous hybrid solutions were

TABLE I
The Recipe of the Preparation of PI/silica Nanocomposite (PI/SiO_2) Materials

Sample name	PAA solution (g)	Silica sol (g)					Film composition (wt %)		[b]Appearence
		TEOS (g)	GOTMS (g)	H_2O (g)	HCl (g)	EtOH (g)	PI	[a]SiO_2	
PI	10.0	–	–	–	–	–	100	0	T
PI/SiO_2-5	10.0	0.28	0.09	0.097	0.026	0.074	95	5	T
PI/SiO_2-10	10.0	0.58	0.19	0.115	0.051	0.156	90	10	T
PI/SiO_2-15	10.0	0.92	0.3	0.182	0.084	0.248	85	15	T
PI/SiO_2-20	10.0	1.3	0.42	0.258	0.117	0.352	80	20	T

[a] Weight percent of total silica in the hybrids, as calculated from the initial amounts of TEOS and GOTMS, assuming complete reaction.
[b] T = transparence.

cast on to glass panels using 30 μm wire gaged applicator and then thermal imidization was performed stepwise at 80, 100, 150, 200, and 300°C for 1 h at each temperature. To obtain free films, the cured films were peeled off from the glass substrate by immersing in distilled water at 80°C. Finally, a series of PI/SiO_2 nanocomposite coating materials were acquired. The preparation flow chart of PI-silica hybrids and their compositions were described in Figure 1 and Table I, respectively.

Measurments

FTIR spectra were recorded on Shimadzu 8303 FTIR Spectrometer. ^{1}H-NMR and ^{31}P-NMR spectra were recorded using a Varian Model T-60 NMR spectrometer operated at 500 MHz.

Thermogravimetric analyses (TGA) of PI/SiO_2 hybrid materials were performed using a TA Instruments Q50 model TGA. Samples were run from 30 to 800°C with a heating rate 10°C/min under nitrogen atmosphere.

The solid state Si-cross-polarization (CP)/magic-angle-spinning (MAS) NMR spectra were recorded using a Varian Unity Inova Spectrometer operated at 500 MHz frequency

Scanning electron microscopy was performed on a JOEL JSM-5910 LV to investigate the morphologies of fractured surfaces of the nanocomposite materials. The fractured surfaces were coated with a gold layer by vacuum sputtering. Moreover, the distributions of Si atoms in the hybrid systems were obtained by SEM EDX mapping (JOEL JSM-5910 LV)

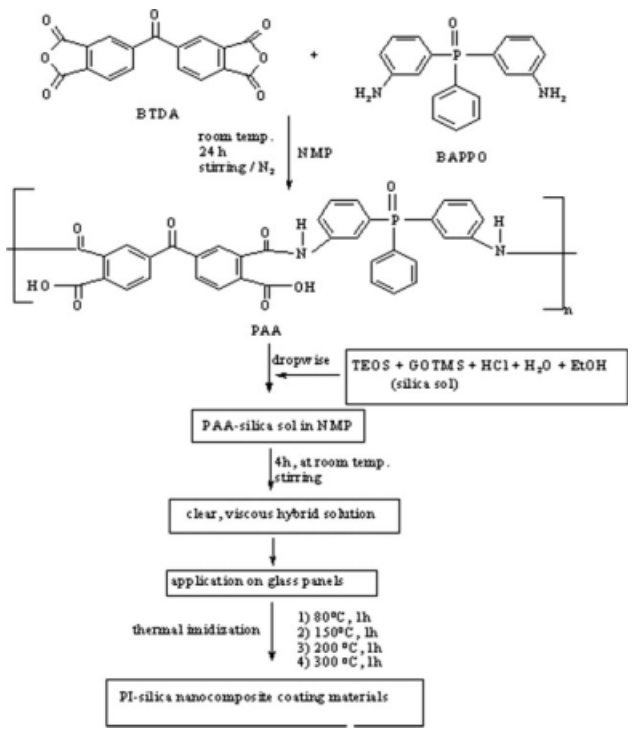

Figure 2 The flow chart for preparation of PI-silica nanocomposite materials containing phenylphosphine oxide.

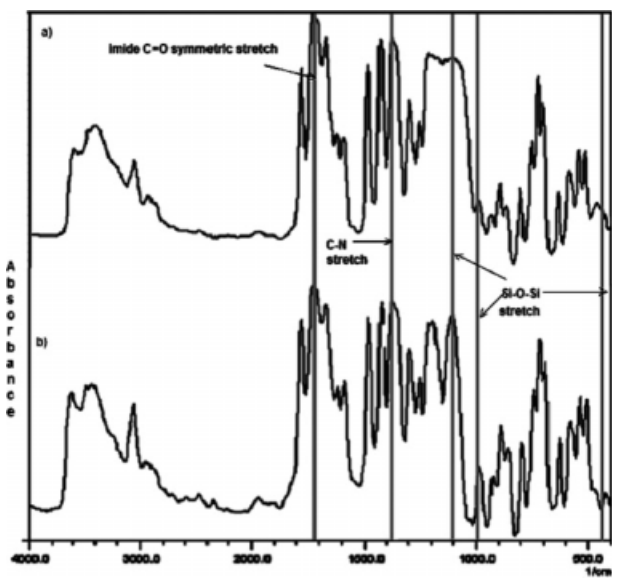

Figure 3 FTIR spectra of **(a)** the polyimide containing phosphine oxide **(b)** polyimide-silica nanocomposite containing 10 wt % silica content.

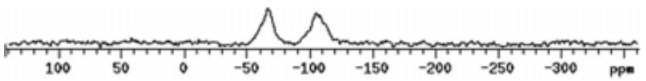

Figure 4 29Si-NMR spectrum of the PI/SiO_2 hybrid material with 10 wt % silica content.

The stress–strain behavior at room temperature was to study A universal test machine (Zwick Rolle, 500 N) with a crosshead speed of 3 mm/min. The measurements represent the average of at least four runs. A König pendulum hardness tester was used to measure the hardness of the nanocomposite materials. The recorded values were on average of four measurements. Contact angle measurements were carried out with a Krüss FM41 instrument, equipped with a camera. Analyses were made at room temperature by means of the sessile drop technique. For each sample, at least three measurements were made and the average was taken. The measuring liquid was distilled water.

UV-visible transmission spectra of the free nanocomposite films were examined in the wave length range of 200–800 nm using a Schimadzu UV 6010 spectrometer.

RESULTS AND DISCUSSION

In this study, a series of novel PI/SiO_2 nanocomposite materials containing phenylphosphine oxide moiety were prepared by sol-gel process. For this, The Figure 1 shows the synthesis of BAPPO (aromatic diamine) monomer. Then, in Figure 2 the preparation of PI/SiO_2 nanocomposite materials from poly (amic acid, PAA) solution (BTDA and BAPPO in NMP), and sol-gel precursor (TEOS, GOTMS) is shown. The poly(amic acid), which is the the polyimide (PI) precursor, was used as an organic polymer matrix in the hybrid system. Besides that, TEOS and GOTMS act as an inorganic network and a coupling agent respectively. The pH of the silane sol was between 4 and 5. Totally, four samples with each have different amounts of sol-gel precursor, in the range of 5–20 wt %, were prepared and characterized. The recipe of preparation of PI/silica nanocomposite (PI/SiO_2) materials is given in Table I.

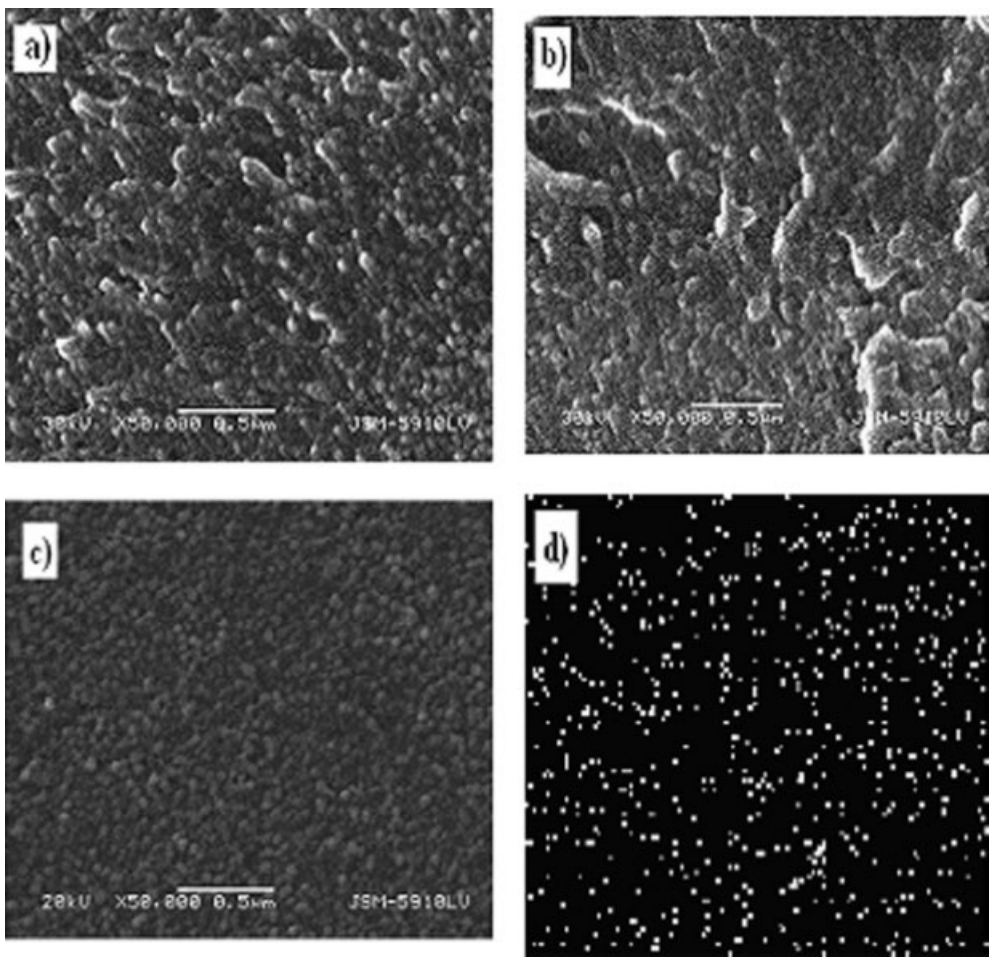

Figure 5 SEM micrographs of (a) PI/SiO_2-5 (b) PI/SiO_2-10 (c) PI/SiO_2-15 (d) Si mapping of PI/SiO_2-15.

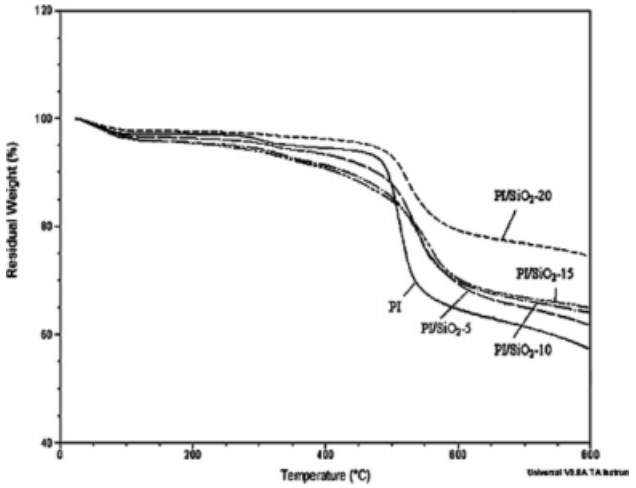

Figure 6 TGA curves of PI and PI/SiO_2 hybrid nanocomposite materials with different silica content.

The apperance of the nanocomposite films was transparent and yellow in color.

The FTIR spectra of the pure PI and PI/SiO_2 nanocomposite (containing 10 wt % silica) films are shown in Figure 3 (a,b). As can be seen in Figure 3(a), it exhibits characteristic imide absorptions at 1780 cm^{-1} and 1725 cm^{-1} (typical of imide carbonyl asymmetrical and symmetrical stretch is respectively), at 1380 and 745 cm^{-1} (C—N—C stretching and imide ring deformation).[12,31] Besides that, the FTIR spectrum consists of other peaks located at 1424 cm^{-1} for aromatic C—P stretching and at about 1300 cm^{-1} for P=O stretching.[30] The mentioned peaks emerge from a BAPPO monomer. As shown in Figure 3(b), when the inorganic components were introduced into the polyimide matrix, the strong absorption bands were observed at the range of 1000–1100 cm^{-1} and 452 $cm^{-1.}$ These bonds were ascribed to the characteristic Si—O—Si stretching vibration and bending vibration respectively.[32] As can be pointed out from the spectra given in Figure 3 (a,b), the absorption bonds related to PI and PI/SiO_2-10 nanocomposite verify the formation of the expected structures.

TABLE II
Thermal Decomposition Temperatures of PI and PI/SiO_2 Nanocomposite Coating Materials

Sample	First weight losses (°C) (T_{1st})	Maximum weight loss (°C) (T_{max})	Char yield (wt %) (800°C)
PI	300	510	57
PI/SiO_2-5	350	550	62
PI/SiO_2-10	350	545	64
PI/SiO_2-15	350	550	65
PI/SiO_2-20	410	530	75

The extent of polycondensation reactions of the alkoxy silane compounds was investigated by ^{29}Si-NMR spectroscopy. The ^{29}Si-NMR spectrum of the PI/SiO_2 nanocomposites coating material containing 10 wt % silica was displayed in Figure 4. As can be seen the figure, mainly two kinds of signals were observed at approximately –65 and 110 ppm corresponding to T^3, and Q^4 peaks, respectively. Q^4 species at −110 ppm is one in which the Si atom is capable of producing four siloxane bonds [$Si(OSi)_4$] and T^3 species at −65 ppm is one which can only achieve three siloxane bonds [R_1 Si $(OR)_3$]. These results might be attributed to the fact that all the hydroxyl groups of the alkoxysilane compounds (TEOS and GOTMS) took part in the condensation reaction in order to form Si—O—Si bonds of the inorganic backbone.[33]

It is known that in polymeric nanocomposite materials compatibility of organic polymer and inorganic part greatly affects the thermal, mechanical, and optical properties. For that reason, surface morphology of the hybrid coating materials is of great importance for many technical applications.[4] The morphologies of the fractured surfaces of the hybrid films with different silica content were investigated by SEM. In Figure 5 (a–c), it can be observed that silica particles are homogenously dispersed through the polyimide matrix. It is clearly seen from the Figure 5(a–c), the silica particles diameter look almost same (30–55 nm). In addition, Figure 5(d) shows Si mapping of PI/SiO_2-15 hybrid material. The white

TABLE III
Mechanical Properties of PI and PI/SiO_2 Hybrid Nanocomposite Materials

Sample	[a]SiO_2 (wt %)	Tensile modulus (GPa)	Tensile strength (MPa)	Elongation at break (%)
PI	0	1.71	63.00	6.24
PI/SiO_2-5	5	2.25	55.00	5.10
PI/SiO_2-10	10	2.37	35.00	4.70
PI/SiO_2-15	15	2.51	27.00	2.30
PI/SiO_2-20	20	ND	ND	ND

ND: Not detected.
[a] Weight percent of total silica in the hybrids, as calculated from the initial amounts of TEOS and GOTMS, assuming complete reaction.

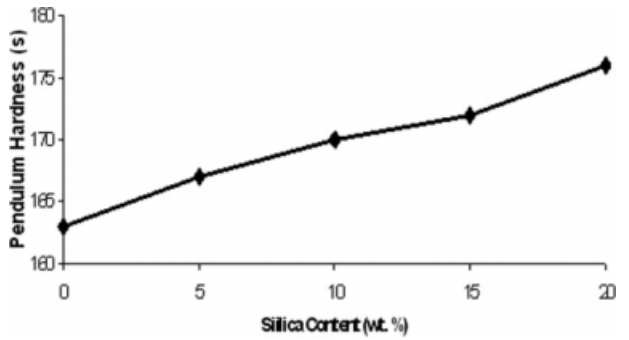

Figure 7 The influence of silica content on the hardness of the PI/SiO_2 nanocomposite coatings.

points in the figure denote Si atoms. According to the figure, the particles were uniformly dispersed throughout the polyimide matrix with sizes around 55 nm. These result can be attributed the fact that the hybrid films showed good interaction interface between the silica particles and the PI matrix.[22,34]

The thermal stability of the PI/SiO_2 nanocomposite coating materials with various silica contents was evaluated by thermogravimetric analysis (TGA) under nitrogen atmosphere as shown in Figure 6. Evaluated TGA data of the nanocomposite materials and pure polyimide are also collected in Table II. From Figure 6, one can see that a slight weight losses (5 wt %) occur around 250°C for all samples due to the evaporation of residual solvents such as NMP, ethanol, and physically absorbed water. The weight loss observed at 300°C for pure PI can be assigned to incomplete imidization. As shown in the Figure 6, TGA curves of the nanocomposite materials exhibited two main weight loss temperatures. First weight loss is due to the degradation of phosphine oxide moiety.[35] Finally, the maximum weight loss observed between 510 and 550°C indicates the decomposition of the polymer. It is observed that the final weight loss peaks for 5–20 wt % silica containing nanocomposite coatings are shifted to higher temperatures compared to the neat polyimide, owing to the fact that the inorganic Si—O—Si linkages in the hybrid systems inhibited the heat and oxygen diffusion. That is why, the decomposition temperature of organic part (PI matrix) is lifted up towards higher values. As can be seen in the Table II, the char yields of the pure polyimide (PI) and PI/SiO2 nanocomposites (PI/SiO_2-5, PI/SiO_2-10, PI/SiO_2-15, PI/SiO_2-20) are 57 and 62, 64, 65, 75, respectively. It is also known that, while burning, the phosphorus riched residue form a glassy layer above the coating and this inhibits the oxygen transfer through the polymer bulk and also limits the production of combustible carbon-containing gasses. These results showed that thermal stability of PI improved by the presence of silica network. Because of the formation of nanocomposite PI/silica network, the polyimide chain is presented from degradation at higher temperatures. As can be seen in Table II, calculated SiO_2 for the nanocomposite materials are agree with those of theoretical SiO_2 contents.

The effects of the silica content on the mechanical properties of PI/SiO2 nanocomposite materials were examined by stress-strain measurements and the modulus, ultimate tensile strength and elongation at break were calculated and listed in Table III. The tensile modulus of the nanocomposite films increase linearly with the increasing silica content. Besides that, as can be seen in Table III the values of elongation at break and tensile strength in the nanocomposite decreased gradually with increasing silica

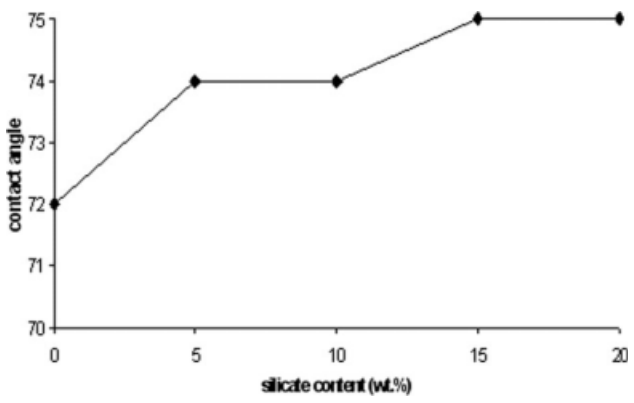

Figure 8 Contact angles of the hybrid coating materials as a function of silica content.

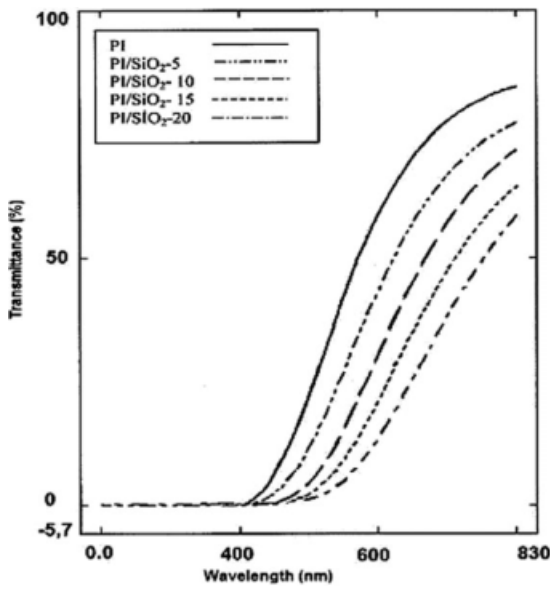

Figure 9 UV-visible transmission spectra of the PI/SiO_2 hybrid coating films.

content. The decrease in elongation may be due to the increased crosslinking density by the formation of organic-inorganic network structure. Under applied stress, since the restricted movement of chains, strain will drastically reduce. These results reveal that the PI/SiO_2 nanocomposite materials are hard and strong compared with pure polyimide. However, when the silica content are up to 20 wt % increased in the nanocomposites, the hybrid nanocomposites are getting brittle due to further increase in crosslinking degree of network. As observed from SEM studies, PI/SiO_2 hybrid materials have nano particle size, and due to the increasing surface area, PI/SiO2 interfacial interchain will be larger. So it makes the nanocomposite structure stiffer than pure PI probably. The improvement of mechanical properties can be explained by the results of formation of the physically crosslinking.[36]

Hardness measurements are a quick, reliable means of quantifying the mechanical properties, and performance of coatings. The hardness of coating is the most significant factor affecting the abrasion and scratch resistance. Smoothness of the coating influences the measurements and also the type of substrate, adhesion to the substrate and heterogeneity within the coating can influence the hardness measurements. Chain flexibility and crosslinking degree of the network play a major role in determination of hardness. In Figure 7 the pendulum hardness of the PI/SiO_2 nanocomposite coating materials as a function of silica content was shown. As can be seen from this figure, incorporation of TEOS and GOTMS into the polyimide matrix gradually improves the hardness. This may result from the strong interfacial interactions between PI matrix and silica particles, which lead to the formation of the physical crosslinking. These results were verified by mechanical tests.

Contact angles are very sensitive to the surface composition changes. the contact angle measurements of the coating materials are the average ones, taken from left and right sides of three droplets. The water contact angles on the glass coating are measured immediately after the drop was settled. As can be seen from the Figure 8, when the sol-gel precursor was added into formation of the polyimide matrix, the contact angles have a slight tendency to increase demonstrating hydrophobic coating surface.

To evaluate the optical transmission, PI/SiO_2 hybrid films were investigated in the wavelength range of 200–800 nm. All the prepared hybrid films are transparent. As can be seen in Figure 9, the introduction of higher silica content into the polyimide matrix, while the values of the transmission were shifted towards the longer wavelengths from 400 to 800 nm, optical transparencies of them decreased.

CONCLUSIONS

In this study, a series of novel polyimide/silica (PI/SiO_2) nanocomposite coating materials containing phenylphosphine oxide with different amounts of silica content, in the range of 5–20 wt % were synthesized by sol-gel technique. The FTIR and ^{29}Si-NMR spectra showed that the fully condensed inorganic network had formed during the imidization. Tensile modulus and hardness of the PI/SiO_2 coating materials increased gradually with increasing inorganic content due to the enhanced interfacial interaction between PI matrix and silica particles. The thermal analysis of the coating materials showed that the degradation of PI was largely reduced with incorporation of silica and also the flame retardancy of the nanocomposite increased. The morphology studies indicated that, the silica particles in the polyimide matrix are dispersed homogeneously and the particle size is in the range of 30–55 nm. Furthermore, it was observed that optical transparencies of the hybrid coating materials decreased due to the introduction of higher silica content into the polyimide matrix and the increasing contact angles demonstrated the formation of hydrophobic nanocomposite surface.

The authors would like to thank PhD. Mustafa İlhan for measurement of Si mapping.

References

1. Chang, T. C.; Wang, G. P.; Tsai, H. C.; Hong, Y. S. Int J Polym Anal Charact 2003, 8, 157.
2. Wen, J. G.; Wilkes, L. Chem Mater 1996, 8, 1667.
3. Zhang, Y. H.; Yan, L.; Fu, S. Y.; Xin, J. H.; Daoud, W. A.; Li, L. F. Polymer 2005, 46, 8373.
4. Karatas, S.; Kayahan-Apohan, N.; Demirer, H.; Güngör, A. Polym Adv Technol 2007, 18, 490.
5. Musto, P.; Ragosta, G.; Scarinzi, G.; Mascia, L. Polymer 2004, 45, 1697.
6. Mascia, L. Trends Polym Sci 1995, 3, 61.
7. Nandi, M.; Conklin, J. A.; Salvati, L.; Sen, A. Chem Mater 1991, 3, 201.
8. Kioul, A.; Mascia, L. J Non-Cryst Solids 1994, 175, 169.
9. Hench, L. L.; West, J. K. Chem Rev 1990, 90, 33.
10. Li, Y.; Fu, S. Y.; Li, Y. Q.; Pan, Q. Y.; Xu, G.; Yue, C. Y. Compos Sci Technol 2007, 67, 2408.
11. Musto, P.; Ragosta, G.; Scarinzi, G.; Mascia, L. Polymer 2004, 45, 4265.
12. Chang, C. C.; Chen, W. C. Chem Mater 2002, 14, 4242.
13. Yen, C. T.; Chen, W. C.; Liaw, D. J.; Lu, H. Y. Polymer 2003, 44, 7079.
14. Marikawa, A.; Yamaguchi, H.; Kakimoto, M.; Imai, Y. Chem Mater 1994, 6, 913.
15. Wang, S.; Ahmad, Z.; Mark, J. E. Chem Mater 1991, 3, 201.
16. Tsai, M. H.; Whang, W. T. Polymer 2001, 42, 4197.
17. Huang, Y.; Gu, Y. J Appl Polym Sci 2003, 88, 2210.
18. Wang, L.; Tian, Y.; Ding, H.; Li, J. Eur Polym J 2006, 42, 2921.
19. Park, H. B.; Kim, J. H.; Kim, J. K.; Lee, Y. M. Macromol Rapid Commun 2002, 23, 544.

20. Musto, P.; Abbate, M.; Lavorgana, M.; Ragosta, G.; Scarinzi, G. Polymer 2006, 47, 6172.
21. Arbash, A. A.; Sagheer, F. A.; Ali, A. A. M.; Ahmad, Z. J Polym Mater 2006, 55, 103.
22. Zhong, S. H.; Li, C. F.; Xiao, X. F. J Membr Sci 2002, 199, 53.
23. Cornelius, C. J.; Marand, E. Polymer 2002, 43, 2385.
24. Delaviz, Y.; Güngör, A.; Mcgrath, J. E.; Gibson, H. W. Polymer 1993, 34, 210.
25. Kwak, S. M.; Yeon, J. H.; Yoon, T. H. J Polym Sci Part A: Polym Chem 2006, 44, 2567.
26. Wang, W.; Wu, Q.; Ding, L.; Yang, Z.; Zhang, A. J Appl Polm Sci 2008, 107, 593.
27. Lee, Y. J.; Güngör, A.; Yoon, T. H.; Mcgrath, J. E. J Adhes 1995, 55, 165.
28. Temple, R. D.; Tsuno, Y.; Leffler, J. E. J Org Chem 1963, 28, 2495.
29. Martinez-Nung, M. F.; Sekharipuram, V. M.; Mcgrath, J. E. Polym Prepr Am Chem Soc Div Polym Chem 1994, 35, 199.
30. Çakir, M.; Karataş, S.; Menceloğlu, Y.; Kayaman-Apohan, N.; Güngör, A. Macromol Chem Phys 2008, 209, 919.
31. Sahao, L.; Liu, L.; Cheng, S. X.; Huang, Y. D.; Ma, J. J Membr Sci 2008, 312, 174.
32. Zhu, Z. K.; Yang, Y.; Yin, J.; Qi, Z. N. J Appl Polm Sci 1998, 73, 2977.
33. Young, S. K.; Jarrett, W. L.; Mauritz, K. A. Polymer 2002, 43, 2311.
34. Wei, S. Q.; Bai, Y. P.; Shao, L. Eur Polym J 2008, 44, 2728.
35. Qiu, F.; Zhou, Y.; Liu, J.; Zhang, X. Optoelectronic Devices Integration; In Proceedings of SPIE; 2005, Vol 5644, p 116.
36. Zhu, Z. K.; Yang, Y.; Yin, J.; Qi, Z. N. J Appl Polym Sci 1999, 73, 2977.